

See discussions, stats, and author profiles for this publication at: <https://www.researchgate.net/publication/231711922>

Gas Transport Properties of Novel Cardo Poly(aryl ether ketone)s with Pendant Alkyl Groups

ARTICLE *in* MACROMOLECULES · JULY 2000

Impact Factor: 5.8 · DOI: 10.1021/ma9921807

CITATIONS

49

READS

26

3 AUTHORS, INCLUDING:



Zhonggang Wang

Dalian University of Technology

502 PUBLICATIONS 10,280 CITATIONS

SEE PROFILE

Gas Transport Properties of Novel Cardo Poly(aryl ether ketone)s with Pendant Alkyl Groups

Zhonggang Wang,^{*,†} Tianlu Chen,[‡] and Jiping Xu[‡]

Institute of Chemistry, Chinese Academy of Sciences, Beijing, 100080, P.R. China, and Changchun Institute of Applied Chemistry, Chinese Academy of Sciences, Changchun, P.R. China

Received December 30, 1999; Revised Manuscript Received April 3, 2000

ABSTRACT: Gas transport of hydrogen, oxygen, nitrogen, carbon dioxide, and methane in four cardo poly(aryl ether ketone)s containing different alkyl substituents on the phenyl ring has been examined from 30 to 100 °C. The permeability, diffusivity, solubility, and their temperature dependency were studied by correlations with gas shape, size, and critical temperature as well as polymeric structural factors including glass transition, secondary transition, cohesive energy density, and free volume. The bulky, stiff cardo and alkyl groups in tetramethyl-substituted TMPEK-C resulted in increased H₂ permeability (by 55%) and H₂/N₂ permselectivity (by 106%) relative to bisphenol A polysulfone (PSF). Moreover, the weak dependence of gas transport on temperature in TMPEK-C made it maintain high permselectivities ($\alpha_{\text{H}_2/\text{N}_2}$ in 68.3 and $\alpha_{\text{O}_2/\text{N}_2}$ in 5.71) up to 100 °C, exhibiting potential for high-temperature gas separation applications.

Introduction

Gas membrane separation technology is useful for a variety of applications,^{1–3} such as hydrogen recovery from reactor purge gas, nitrogen and oxygen enrichment, water vapor removal from air, stripping of carbon dioxide from natural gas, etc. Over the past decade, finding new membrane materials with high permeability and permselectivity has been an active research field.^{4–7} Recent studies indicate that the packing density and segmental motion of the polymer chain are two dominant factors that affect gas transport properties. High permeability is primarily related to high free volume, while significant increases in gas permselectivity may be due to restricted segmental motion.^{8–10} On the basis of these facts, one can design new polymers to combine the two favorable factors, thus preparing polymers with both high gas permeability and high permselectivity.

A review of gas permeability studies revealed that, relative to the numerous papers on the polymer gas transport properties at room temperature, in recent years, research studies on high-temperature gas separation are rather rare. However, from the viewpoint of energy saving, in some cases, e.g. “C₁ chemistry”, it is desirable for the membrane separation process to be operated at the highest allowable temperature, so that the purge streams from synthesis gas production can be regulated in composition and recycled without extensive cooling and reheating prior to recycling to the reactor. Therefore, the effect of temperature on gas permeability is of great importance for membrane separation applications at high temperature.

Phenolphthalein-based poly(aryl ether ketone) (PEK-C) has been noted for its excellent mechanical toughness, thermooxidative stability, and high glass transition temperature. In addition, PEK-C is soluble in a few polar solvents such as DMF, NMP, and chloroform and can be easily cast into a flexible tough film.¹¹ The

experimental results on its gas permeability studies reveal that, in comparison with conventional glassy polymers, such as bisphenol A polysulfone,¹² bisphenol A polycarbonate,¹³ and polyimide (Kapton),¹⁴ PEK-C membranes possess better gas transport properties,¹⁵ but for the purpose of future practical application, its gas selectivity coefficient and permeability coefficient must be further improved.

In our previous paper,¹⁶ several chemical modifications had been performed to incorporate pendant amide and carboxyl groups onto the PEK-C backbone. The enhanced interchain interaction in the polymers, owing to intermolecular hydrogen bonds and ionic bonds, leads to the polymers' extremely high gas permselectivity, but their permeability coefficients also dropped to some extent.

The present paper mainly concerns the gas permeability of a series of newly synthesized poly(aryl ether ketone) membranes over a temperature range from 30 to 100 °C. The systematic variations in chemical structure with different alkyl substituents on the phenylene unit were expected to result in interesting and unique variations in physical properties, e.g., packing density and segmental motion of the polymer chain, and thus would significantly affect the gas permeation behavior in polymer membranes. The effects of alkyl substituents on the gas permeability and their temperature dependency were explained according to wide-angle X-ray diffraction, cohesive energy density, free volume, and dynamic mechanical analysis.

Experimental Section

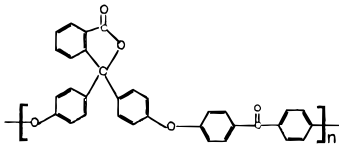
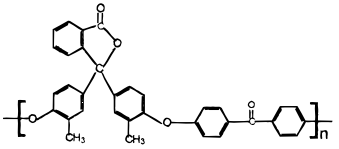
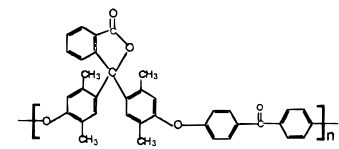
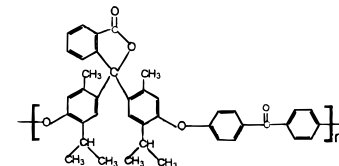
Materials. Phenolphthalein (PPH) and 2',2''-dimethylphenolphthalein (DMPPH) were purchased from Beijing Chemical Works and purified by recrystallization from a 50:50 (v/v) mixture of ethanol and water. Melting points are 262–263 and 220–222 °C, respectively. 2',2'',5',5''-Tetramethylphenolphthalein (TMPPH) and 2',2''-diisopropyl-5',5''-dimethylphenolphthalein (IMPPH) were purchased from Fluka Chemical Corp., with melting points of 239–240 and 251–252 °C, respectively, and were used as received. Bis(4-nitrophenyl) ketone (DNDPK) was prepared in our laboratory, mp 189–190 °C. Dimethyl sulfoxide (DMSO) and *N,N*-dimethylform-

[†] Institute of Chemistry.

[‡] Changchun Institute of Applied Chemistry.

* To whom all correspondences should be addressed.

Table 1. Chemical Structures of the Four Poly(aryl ether ketone)s

Chemical Structure	Abbreviation	$\eta_{\text{RV}}(\text{dl/g})$
	PEK-C	0.663
	DMPEK-C	0.625
	TMPEK-C	0.695
	IMPEK-C	0.518

amide (DMF) were purified by vacuum distillation just before use; anhydrous potassium carbonate was finely powdered prior to use.

All the poly(aryl ether ketone)s studied here were prepared via nucleophilic polycondensation from various bisphenols and DNDPK in the DMSO/ K_2CO_3 system in a similar procedure to that described in ref 17. Their chemical structures as well as reduced viscosity and density data are presented in Table 1.

Film Preparations. The polymer samples were dissolved in 1,1,2-trichloroethane (TCE) at a concentration of 8 wt %. The solution was cast onto a clean glass plate at room temperature. After most of the solvent had evaporated, the films were stripped from the glass plates and transferred to a vacuum oven, where they were first dried at room temperature for 12 h, and then the temperature was increased incrementally to 200 °C and maintained at this temperature and 10 mmHg for 48 h. The film thickness was 35–40 μm .

Measurements. Reduced viscosities were measured using a Ubbelohde viscometer at a concentration of 0.5% (w/v) in DMF at 25 ± 0.01 °C.

Polymer densities were determined in a density gradient column containing aqueous solution of calcium nitrate at 30 °C.

Free volume (V_F) of each of the polymers is given by the equation $V_F = V_T - V_0$, where V_T is specific volume, which can be calculated from the polymer density; V_0 is the polymer occupied volume at 0 K and was obtained according to the group contribution method of Sugden.¹⁸

Wide-angle X-ray diffraction (WAXD) measurements were performed at room temperature (about 25 °C) on a D/Max-B X-ray diffractometer, using Cu K α radiation at a wavelength of 1.54 Å (40 kV, 15 mA). The scanning rate was 2°/min over a range of $2\theta = 5^\circ\text{--}40^\circ$.

Table 2. Gas Transport Properties of Polymers at 30 °C²⁰

polymers	$P_{\text{H}_2}^a$	$\alpha_{\text{H}_2/\text{N}_2}$	P_{O_2}	$\alpha_{\text{O}_2/\text{N}_2}$	P_{CO_2}	$\alpha_{\text{CO}_2/\text{CH}_4}$	$\alpha_{\text{CH}_4/\text{N}_2}$
PEK-C	11.7	75.6	0.95	6.2	2.73	33.2	0.53
DMPEK-C	10.3	95.2	0.87	8.9	2.60	37.1	0.63
TMPEK-C	21.5	114.4	1.55	8.2	5.44	32.0	0.89
IMPEK-C	42.5	45.3	4.85	5.2	19.3	17.7	1.17
PSF ¹²	13.9	55.6	1.4	5.6	5.6	22	1.02

^a P : barrer, 1 barrer = 10^{-10} $\text{cm}^3(\text{STP}) \text{ cm}/(\text{cm}^2 \text{ s cmHg})$.

Dynamic mechanical analysis (DMA) was performed on film samples using RHEOVIBRON-DDV-II-E_A (Japan), at a frequency of 3 Hz and a heating rate of 4 °C/min from –150 to +270 °C. The preparation and posttreatment of the film samples are completely same as that used for the gas permeability measurement.

Pure gas permeability coefficients over the temperature interval from 25 to 100 °C for H_2 , O_2 , N_2 , CO_2 , and CH_4 with an upstream pressure of 5 atm were measured using the apparatus described in the literature.¹⁹ The permeation cell temperature was controlled within ± 0.2 °C and was measured by a calibrated Cu–constantan thermocouple inserted just above the membrane in the permeation cell. To eliminate the CO_2 plasticization effect, CO_2 was measured after the other gases. All the gases used here were at least 99.99% in purity. The permeability coefficient (P) was obtained from the slope of pressure–time plots after steady state has been reached. The apparent diffusion coefficients (D_{app}) were determined using the time lag method according to the relation $D_{\text{app}} = l^2/6L$, where L is the time lag and l is the thickness of the membrane. The solubility coefficients (S) were calculated from $S = P/D$. The ideal separation factor ($\alpha_{A/B}$) of gas A relative to gas B is given by $\alpha_{A/B} = P_A/P_B = (D_A/D_B)(S_A/S_B)$, where P_A and P_B are the permeability coefficients for gases A and B, D_A and D_B are diffusivity coefficients, and S_A and S_B are solubility coefficients. The ratios D_A/D_B and S_A/S_B are known as the diffusivity selectivity and the solubility selectivity, respectively.

Results and Discussion

Gas Transport. The gas permeability data of H_2 , O_2 , N_2 , CO_2 , and CH_4 through these four polymer membranes are summarized in Table 2. In each polymer the permeability of H_2 , having the smallest kinetic diameter, is the highest and is followed by those of the progressively bigger penetrants except for IMPEK-C, which has the slightly higher CH_4 permeability than N_2 . Among the four polymers, dimethyl- and diisopropyl-substituted IMPEK-C exhibited the highest gas permeability. For example, in comparison to the unmodified PEK-C, the permeability coefficients of H_2 , O_2 , and CO_2 in IMPEK-C are higher by 263%, 411%, and 607%, respectively. On the contrary, dimethyl-substituted DMPEK-C displayed decreased gas permeability and increased selectivity.

Generally, the improvement in gas permeability based on chemical structure modifications is accompanied by a sacrifice in gas selectivity. However, the behavior of TMPEK-C, with two methyl substituents on one phenylene unit, is somewhat unusual. It generally displayed increased gas permeability and selectivity coefficients relative to PEK-C. For example, the P_{H_2} and $\alpha_{\text{H}_2/\text{N}_2}$ of TMPEK-C were 84% and 51% higher than those of PEK-C, respectively.

Gas Diffusivity and Solubility. An analysis of the effect of polymer structure on gas permeability requires knowledge of the solubility and diffusivity coefficients in addition to the permeability coefficient. The results of gas diffusivity and diffusivity selectivity as well as gas solubility and solubility selectivity in the four polymers are listed in Table 3 and Table 4.

Table 3. Gas Diffusivity and Diffusivity Selectivity at 30 °C

polymers	$D \text{ (cm}^2\text{/s)} \times 10^{-8}$				D_{O_2}/D_{N_2}	D_{CO_2}/D_{CH_4}
	O ₂	N ₂	CO ₂	CH ₄		
PEK-C	2.15	0.618	0.746	0.0959	3.48	7.78
DMPEK-C	1.96	0.295	0.639	0.0597	6.64	10.7
TMPEK-C	3.31	0.516	1.22	0.142	6.41	8.57
IMPEK-C	9.12	2.25	3.83	0.634	4.06	6.04

Table 4. Gas Solubility and Solubility Selectivity at 30 °C

polymers	$S \text{ (cm}^3 \text{ (STP))/(cm}^3 \text{ atm)}$				S_{O_2}/S_{N_2}	S_{CO_2}/S_{CH_4}
	O ₂	N ₂	CO ₂	CH ₄		
PEK-C	0.336	0.238	2.78	0.651	1.41	4.27
DMPEK-C	0.337	0.246	3.09	0.828	1.34	3.73
TMPEK-C	0.356	0.276	3.40	0.980	1.29	3.47
IMPEK-C	0.405	0.316	5.03	1.717	1.28	2.93

Table 5. Gas Physical Properties

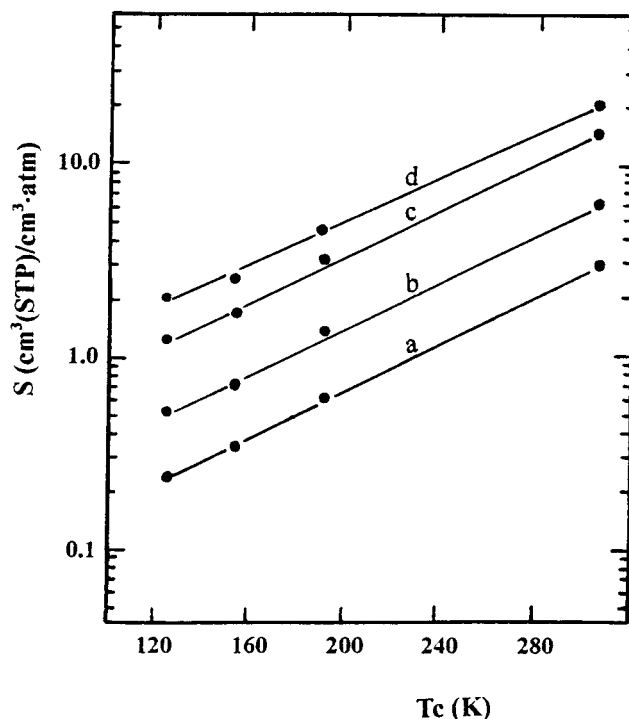
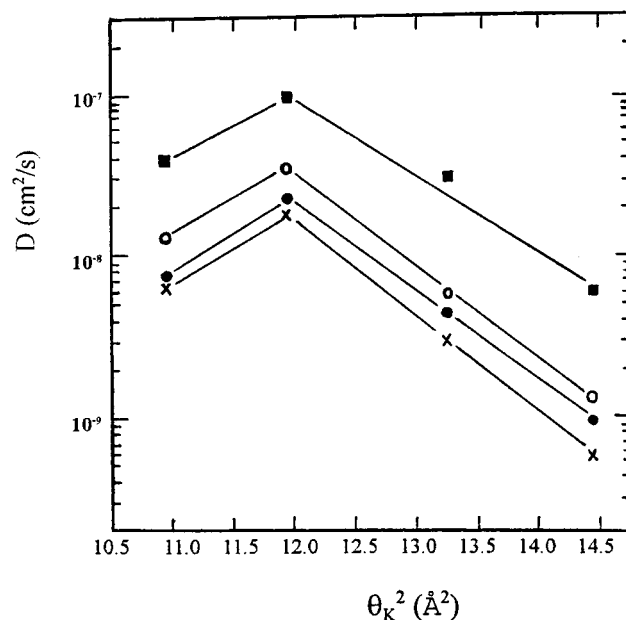
gases	critical temp ²¹ $T_c \text{ (K)}$	kinetic diameter ²² $\theta_K \text{ (Å)}$	collision diameter ²³ $\theta_C \text{ (Å)}$
H ₂	33.2	2.89	2.83
CO ₂	304.2	3.30	3.95
O ₂	154.6	3.46	3.47
N ₂	126.2	3.64	3.80
CH ₄	190.6	3.80	3.76

The gas physical properties are given in Table 5. The higher the T_c , the higher the solubility coefficient. For each of the polymers, $\log S$ was observed to linearly increase with T_c . This correlation was consistent with that reported in a number of references.^{24–26}

The relationship between gas diffusion coefficient ($\log D$) and gas molecular kinetic diameter (θ_K) is shown in Figure 2. For O₂, N₂, and CH₄, which have similar critical temperatures, a straight line is obtained, and gas diffusivity decreases with increasing penetrant size. Despite CO₂ smaller molecule size, its diffusivity coefficient is far lower than that of O₂, due to the energetically favorable interaction of CO₂ with the large number of polar groups in the polymer, and these polar groups act to impede its diffusion.^{27,28}

According to the "solution–diffusion" mechanism,²⁹ gas permeability depends on both the gas diffusivity and solubility. However, the diffusion and solution behavior of one gas is quite different from that of another, so that the respective contribution of diffusion and solution factors to permeability is decided by the specific gas pair studied. As revealed in Tables 3 and 4, for relatively uncondensable O₂ and N₂, the O₂/N₂ diffusivity selectivity in the four polymers varied from 3.48 to 6.64, whereas its solubility selectivity was only about 1.3. Therefore, the O₂/N₂ permeability and selectivity coefficients were primarily dominated by the diffusivity factor, whereas for CO₂ and CH₄, CO₂ displayed obviously higher solubility coefficients so that the solubility and solubility selectivity factors played a significantly increased role in permeability and permselectivity of CO₂ over CH₄.

Structure–Property Relations. The incorporation of alkyl substituents on the phenyl ring of PEK-C resulted in significant variations in physical characteristics such as free volume and cohesive energy density (CED), glass transition, and secondary transition temperature. As shown in Figure 3, in the temperature range from $-150 \sim +270$ °C, all of the polymers exhibited three transitions, labeled as α , β , and γ in the order from high to low temperature, respectively. The α transition corresponds to the onset of long-scale molec-

**Figure 1.** Relationship of $\log S$ vs T_c in the four polymers (a) PEK-C, (b) DMPEK-C $\times 2$, (c) TMPEK-C $\times 4$, and (d) IMPEK-C $\times 6$.**Figure 2.** Plots of $\log D$ vs penetrant size (θ) for these polymers: (x) DMPEK-C; (●) PEK-C; (○) TMPEK-C; (■) IMPEK-C.

ular motion associated with the glass transition (T_g). As seen in Table 6, compared to PEK-C, DMPEK-C and IMPEK-C revealed slightly lower T_g values (239 and 241 °C, respectively), whereas TMPEK-C showed a higher T_g (266 °C).

In the temperature range of gas permeability studied here, all of the polymers were glassy and their long-scale polymer segmental motion had been frozen, but secondary transitions that occurred at lower temperature were still active. Therefore, the polymer permeability might be closely related to the secondary transition. Since all the film samples had been treated by

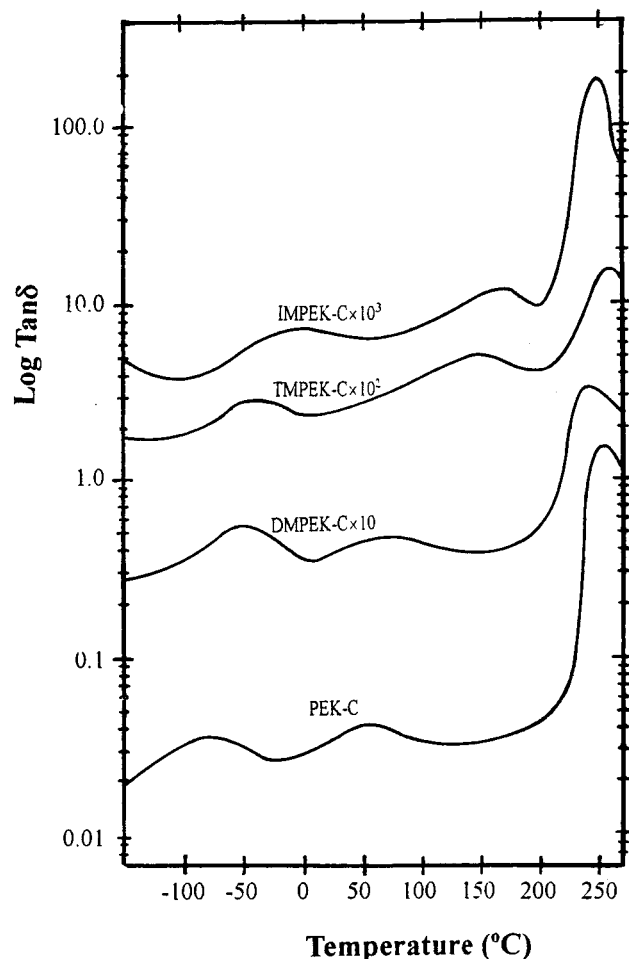


Figure 3. Log tan δ as a function of temperature for the four polymers.

Table 6. Physical Properties of Polymers

polymers	$T_g/^\circ\text{C}$	$T_\beta/^\circ\text{C}$	$T_\gamma/^\circ\text{C}$	$V_F^{20}/(\text{cm}^3/\text{g})$	$\text{CED}^{20}/(\text{kJ}/\text{cm}^3)$
PEK-C	249	53.3	-80.5	0.124	458.4
DMPEK-C	239	63.2	-50.3	0.112	474.8
TMPEK-C	266	147.1	-41.8	0.131	429.1
IMPEK-C	241	166.2	+3.95	0.159	418.6

annealing, the β and γ transitions did not result from packing defects among the polymer chains but are attributed to the small molecule unit rotational movement around the flexible bond in the polymer chain. In substituted cardo poly(aryl ether ketone)s, the β transition is ascribed to the rotations of the substituted phenyl ring about the C-C bond, and the γ transition is associated with the unsubstituted phenyl rings around the C-O bond.³⁰

The substitution of phenylene hydrogens with methyl and isopropyl groups hindered the intrachain rotational motion considerably. As shown in Table 6, relative to PEK-C, the methyl substitution made TMPEK-C and IMPEK-C exhibit higher β transition by 93.8 °C and 112.9 °C, respectively. The β transition of DMPEK-C was found to be only slightly higher than that of PEK-C because there is no substituent ortho to the C-C bond. The γ transitions of DMPEK-C, TMPEK-C, and IMPEK-C, with methyl or isopropyl substitution ortho to the ether bond, increased from -80.5 °C of PEK-C to -50.3, -41.3, and +3.95 °C, respectively.

Wide-angle X-ray diffractograms of the four polymers are illustrated in Figure 4. All of the polymers are

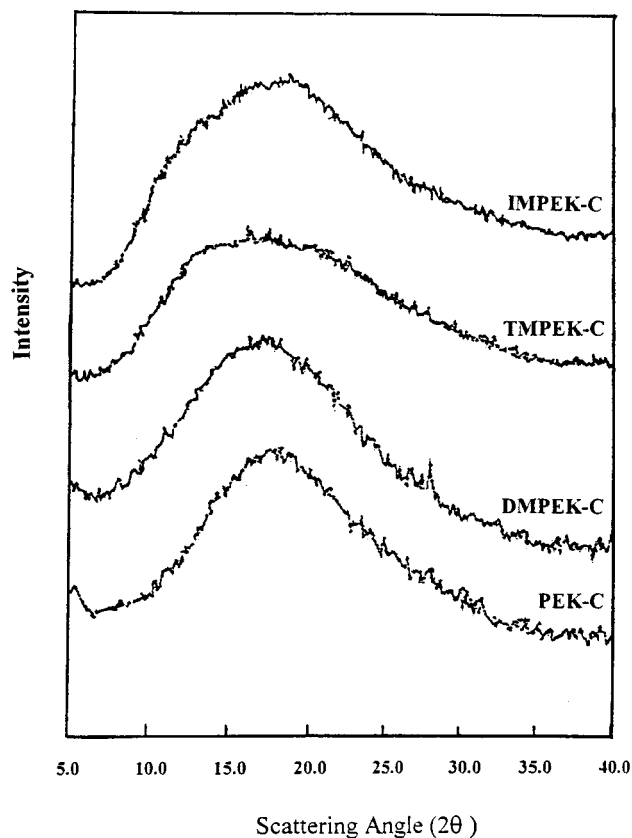


Figure 4. WAXD patterns of the polymer membranes.

amorphous due to the presence of the packing disruptive cardo phthalide groups and alkyl substituents. It can be seen from Figure 4 that PEK-C and DMPEK-C had a similar diffraction pattern, but the patterns for TMPEK-C and IMPEK-C were broadened considerably, suggesting that the packing regularity of the polymers decreased greatly with the increase in number and size of alkyl substituents.

The free volume generally can be used as a measure of polymer chain packing density or the "tightness" of the polymer structure, while CED can be used as an indicator of interaction of polymer chains and facility of segmental motion. The cohesive energy densities (CED), calculated according to the group contribution method,³¹ and free volumes (V_F) are presented in Table 6. High V_F is more favorable for polymer segmental motion, and the CED order (from high to low) is opposite to the order of V_F . When only one phenyl hydrogen atom ortho to the ether bond was replaced by a methyl group, the relatively small methyl group is not enough to force the polymer chain apart but may occupy the free volume space between polymer chains. Consequently, the dimethyl-substituted DMPEK-C exhibited lower V_F (by 9.7%) and higher CED (by 3.6%) than that of PEK-C. TMPEK-C, which had two phenyl hydrogens meta and ortho to the ether bond substituted by methyl groups, displayed completely different packing density behavior from that of DMPEK-C. Its free volume increased by 5.6% and CED decreased by 6.4% compared to that of PEK-C. As expected, the bulky isopropyl substituted polymer IMPEK-C has the highest free volume and lowest cohesive energy density among the four polymers.

The gas permeability through the four polymers can be clearly understood by correlating it with the polymer

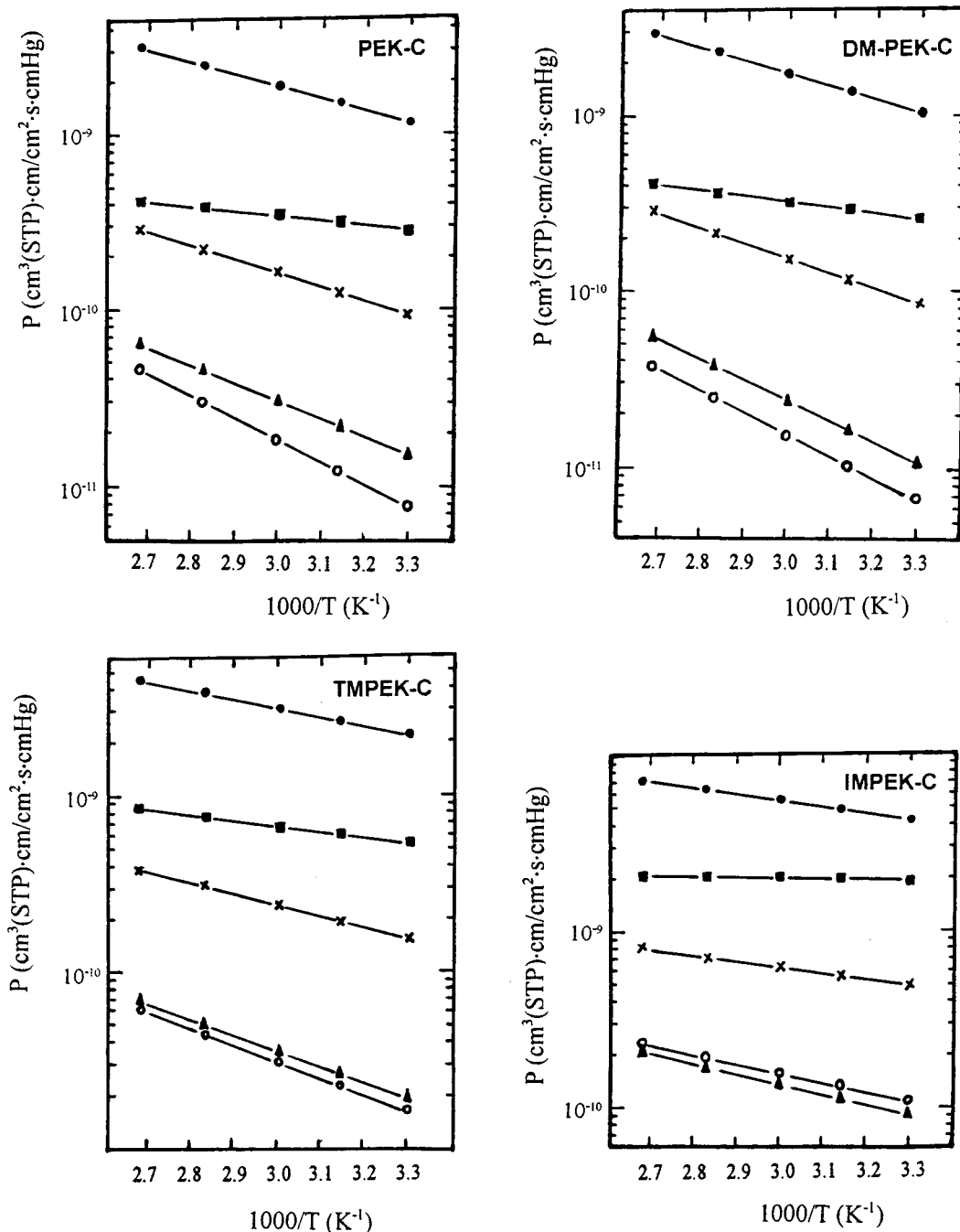


Figure 5. Plots of gas permeability as a function of temperature: (●) H₂; (■) CO₂; (×) O₂; (▲) N₂; (○) CH₄.

structure data. Compared to the unsubstituted PEK-C, DMPEK-C had simultaneously increased polymer chain packing density and molecule rotation hindrance around the flexible linkage. Both of these factors were disadvantageous for gas diffusion but favorable for gas diffusion selectivity, resulting in the DMPEK-C membrane the lowest permeability coefficients and the highest selective coefficients for O₂/N₂ and CO₂/CH₄. For TMPEK-C, the high free volume was very advantageous for gas diffusion, especially for the smaller gas molecules such as H₂, O₂, and CO₂. But, the methyl substitution meta and ortho to the C–O bond severely restricted the phenylene unit rotation motion so that accessible free volume elements in the polymer were more difficult to open to allow gas molecules of bigger size to jump from one “hole” to another. Therefore, TMPEK-C revealed both high permeability due to its high free volume and

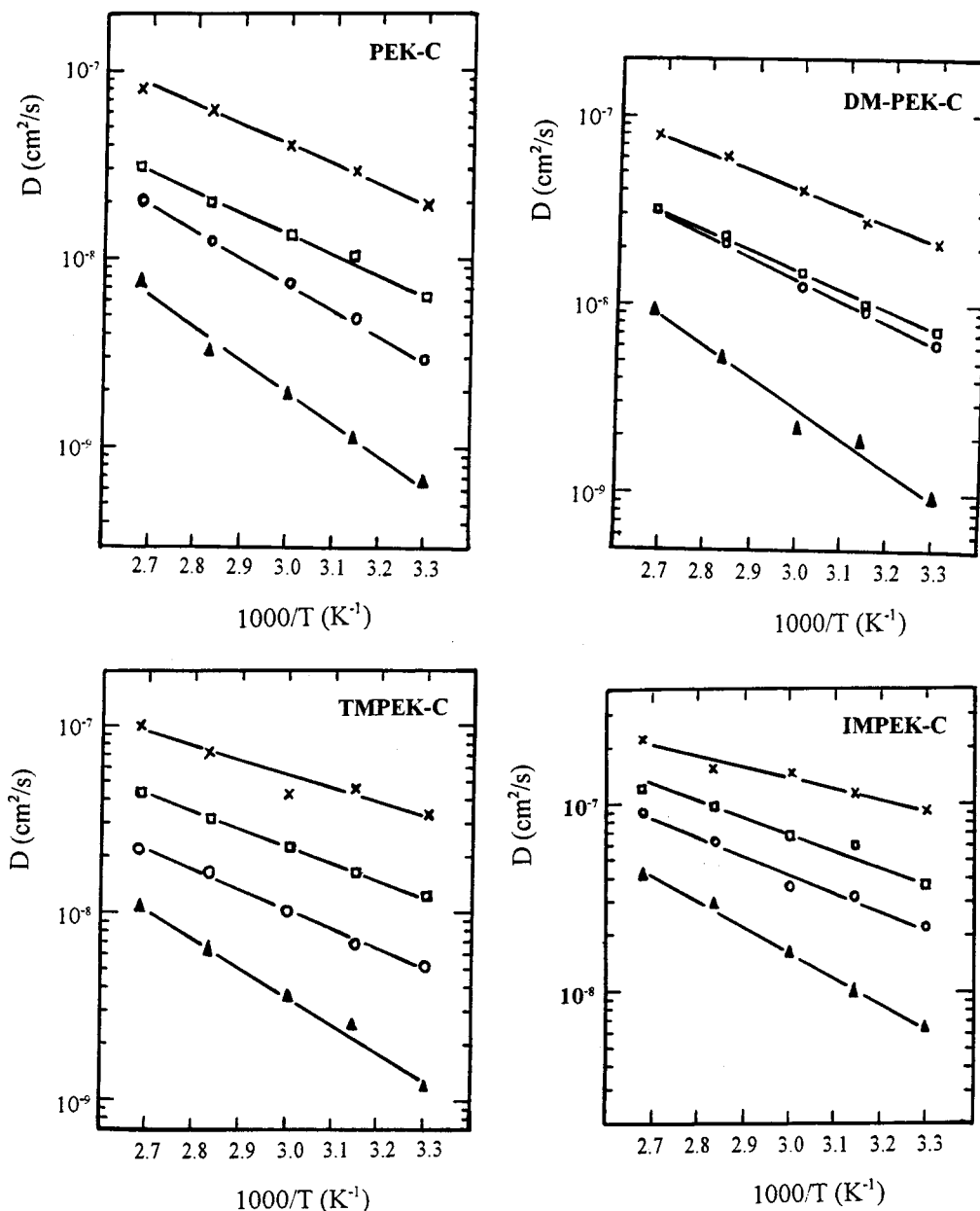
high permselectivity due to its low intrachain rotation ability. For IMPEK-C, its intrachain rotation was also inhibited, but the factor of free volume may play a dominant role in gas permeability. As a result, its gas permeability increased significantly but permselectivity decreased.

Temperature Dependency. The curves of $\log P$ vs $1/T$ for the four polymers are given in Figure 5. In the temperature range 30–100 °C, the relationships of gas permeabilities and temperature were consistent with the Arrhenius equation $P = P_0 e^{-E_p/RT}$, where P_0 is a preexponential factor, R is the gas constant, and E_p is the apparent activation energy.^{27,32}

The E_p values for the five gases were calculated from the slope of Arrhenius plots. These values and the permeability at 60 and 100 °C are listed in Table 7. Similar to other polymers, these four polymers also show

Table 7. Apparent Activation Energy and Gas Transport Properties at 60 and 100 °C

polymers	E_p (kJ/mol)					60 °C				100 °C			
	H ₂	O ₂	N ₂	CO ₂	CH ₄	$P_{H_{2a}}$	α_{H_2/N_2}	P_{O_2}	α_{O_2/N_2}	P_{H_2}	α_{H_2/N_2}	P_{O_2}	α_{O_2/N_2}
PEK-C	13.3	14.9	19.3	5.43	22.9	12.0	57.6	1.50	5.08	31.5	48.9	2.88	4.48
DMPEK-C	14.1	16.2	21.6	5.94	22.4	15.6	68.4	1.45	6.37	29.4	54.5	2.91	5.39
TMPEK-C	9.70	11.7	16.6	5.58	16.8	26.2	82.1	2.09	6.56	44.3	68.3	3.70	5.71
IMPEK-C	6.84	6.69	10.4	1.32	9.82	43.3	36.7	4.98	4.18	64.4	31.8	7.99	3.94

^aP: barrer.**Figure 6.** Plots of gas diffusivity as a function of temperature: (□) CO₂; (×) O₂; (▲) CH₄; (○) N₂.

increased permeability and decreased permselectivity with increasing temperature. The E_p 's in this series of polymers were in the order DMPEK-C > PEK-C > TMPEK-C > IMPEK-C. For the five gases, E_p 's were in the order CH₄ > N₂ > O₂ > H₂ > CO₂. Among the four polymers, DMPEK-C and IMPEK-C exhibited the highest and the lowest temperature dependency, respectively. It should be noted that, even though the temperature was increased to 100 °C, TMPEK-C still maintained a high gas selectivity (α_{H_2/N_2} of 68.3 and α_{O_2/N_2} of 5.71), which were higher than that of Bisphenol A polysulfone (PSF)¹² at 35 °C. This characteristic is

very useful for high-temperature gas separation applications.

To elucidate the relationship between temperature dependency and polymer structure, Arrhenius plots (log D vs $1/T$) for the diffusivity of CH₄, CO₂, O₂, and N₂ through the polymers are shown in Figure 6. The apparent diffusion activation energies were calculated from the slopes. The heats of solution for these gases were obtained by the equation $H_s = E_p - E_D$.^{27,32}

As shown in Table 8, among the four gases, CH₄ exhibited the highest diffusion activation energy because it was the largest molecule considered. The strong

Table 8. Apparent Diffusion Activation and Solution Heat

polymers	E_D (kJ/mol)				H_s (kJ/mol)			
	O ₂	N ₂	CO ₂	CH ₄	O ₂	N ₂	CO ₂	CH ₄
PEK-C	17.6	22.4	19.5	30.1	-2.70	-3.14	-14.1	-7.15
DMPEK-C	20.7	26.5	20.8	33.7	-4.52	-4.90	-14.9	-11.3
TMPEK-C	13.7	19.2	17.2	26.7	-2.01	-2.61	-11.6	-9.89
IMPEK-C	11.4	18.7	16.9	26.3	-4.74	-8.30	-15.6	-16.5

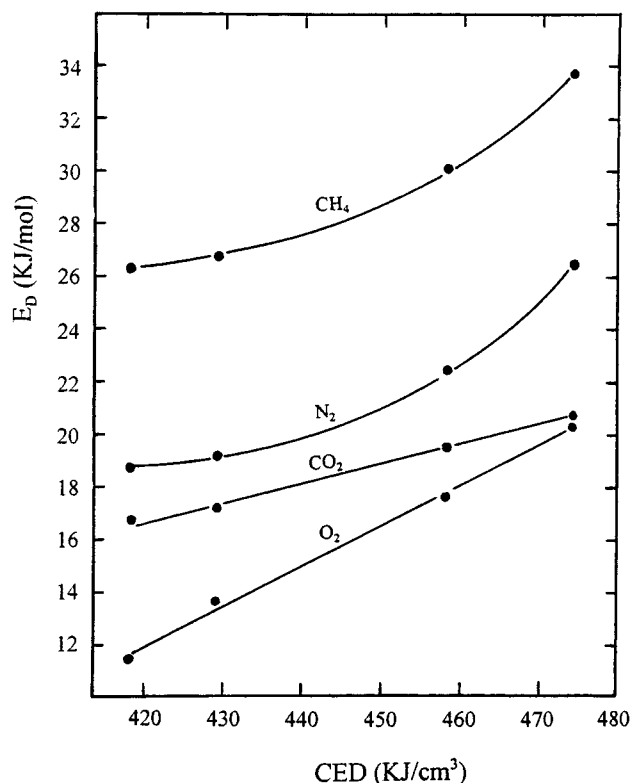
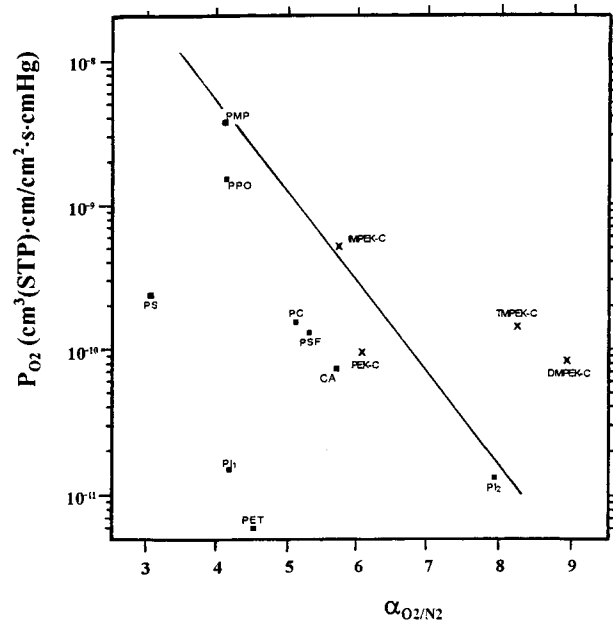
affinity of CO₂ for the polymer chains, which was reflected in its large negative heat of solution, greatly inhibited its diffusion through polymer membrane, leading to higher E_D values than those of O₂ although the θ of CO₂ is smaller than that of O₂.

According to Meares's gas diffusion model, gas diffusion takes place along a somewhat cylindrical volume $(\pi/4)\delta^2\lambda$, which is related to the thermal-energy-induced segmental motions as well as shape and size of the gas molecules. Here δ is the diameter of the cylinder, and λ is the diffusional length. On the basis of this hypothesis, he equated E_D to the product of CED and the volume of the diffusional cylinder as $E_D = (\pi/4)\delta^2\lambda(\text{CED})$.^{33,34}

As a measure of the size of gas molecules, kinetic diameter and Lennard-Jones collision diameter are usually used. The kinetic diameter is the calculated value, equal to the intermolecular distance of two molecules collision with zero initial kinetic energy, and is taken to respond to the smallest diameter that allow the given gas molecule to enter the inner cavity. The collision diameter is often determined from viscosity data and, therefore, is an average dimension over all possible orientations. As shown in Table 5, the differences between gases collision diameter and kinetic diameter are very small except for CO₂, which has the largest collision diameter among the gases studied. Considering the fact that CO₂ has the larger diffusion coefficient in this series of polymers as well as in many other glassy polymers, it is reasonable to take kinetic diameter rather than collision diameter to represent the cylinder diameter of Meares's model.

The plots of E_D vs CED of polymers for O₂, CO₂, N₂, and CH₄ are shown in Figure 7. For the smaller gas molecules such as O₂ and CO₂, satisfactory linear relationships were observed between E_D and CED. But for the larger gas molecules such as N₂ and CH₄, the plots of E_D vs CED obviously curved upward, indicating that the larger gas molecules were more sensitive than the smaller gases. In the case of the four poly(aryl ether ketone)s studied here, the cardo phthalide group and alkyl substituents on the phenylene unit lead to very stiff polymer chains. For smaller gases, the passage way may be sufficient, and only low levels of segmental motion energy were needed for gas molecules diffusion, whereas for larger gas molecules, more energy was required to diffuse through a stiff polymer matrix, resulting in positive deviation from Meares's equation. The slope of CO₂ was seen to be lower than that of O₂, indicating that CO₂ had a relatively small diffusional diameter. A possible reason for this may result from the fact that CO₂ has a straight-line-shaped molecule structure, and the kinetic diameter of CO₂ is also smaller than that of O₂.

Transport Property Evaluation. The polymers in this study exhibited simultaneously higher permeability and permselectivity, as can be seen in the O₂/N₂ tradeoff curve in Figure 8 for a representative group of commercial polymers used for gas separation, as well as for

**Figure 7.** Relationship between E_D and CED for the four polymers.**Figure 8.** Tradeoff curve of P_{O_2} vs α_{O_2/N_2} .²⁰ PSF = bisphenol A polysulfone;¹² PC = bisphenol A polycarbonate;¹³ CA = cellulose acetate;³⁵ PET = poly(ethylene terephthalate);³⁶ PI₁ = polyimide (Ube);³⁷ PI₂ = polyimide (Kapton);³⁸ PMP = poly(4-methylpentene-1);³⁹ PS = polystyrene;⁴⁰ PPO = poly(phenylene oxide).⁴¹

the poly(aryl ether ketone)s in this study. Typically, highly permeable polymers always exhibit low gas selectivity, and vice versa. For example, polyimide (Ube) has a high selectivity but a relatively low permeability, while poly(phenylene oxide) has high permeability but low selectivity. However, for the newly synthesized substituted cardo poly(aryl ether ketone)s, all of them were found to be in the upper-right region relative to

the conventional polymers. IMPEK-C has O_2 permeability of 4.9 barrers, over twice as higher that of PSF with a comparable O_2/N_2 separation factor. The H_2 and O_2 permeability of TMPEK-C are 54% and 10.7% higher than that of PSF, while its H_2/N_2 and O_2/N_2 separation factors are also increased by 106% and 46%, respectively.

Conclusion

The above study clearly demonstrated that polymer design for specific applications in gas separation could be achieved by variation of structural factors such as free volume, cohesive energy density, mobility of polymer chain segments, intrachain rotational mobility, etc. Similar to most glassy polymers, for the uncondensable O_2/N_2 gas pair, the gas permeability behavior in the four polymers was primarily governed by diffusivity and diffusivity selectivity. On the contrary, for CO_2/CH_4 , high CO_2 solubility leads to an increased contribution of solubility selectivity to gas permeability and permselectivity of CO_2 over CH_4 .

The gas permeability through the four cardo polymers was greatly affected by the number, position, and size of the alkyl substituents. The dimethyl substitution seemed to result in DMPEK-C a specific chain orientation so that the relatively small methyl may occupy between the polymer chains, and this was responsible for the DMPEK-C high permselectivity and low permeability. TMPEK-C displayed both high permeability and permselectivity owing to its loose packing density and severely inhibited intrachain rotation. The highest free volume among the four polymers made IMPEK-C 4 times more permeable than PEK-C with correspondingly decreased permselectivity.

The gas permeability temperature dependency was studied according to the gas permeation apparent activation energy, diffusion activation, and solution heat. The results revealed that the solution heat was mainly determined by the gas critical temperature, and the diffusion activation energy was dependent on the free volume, segmental mobility, and the gas molecule shape and size. The combination of excellent permeation and separation properties at room temperature and fairly low temperature dependency made TMPEK-C display O_2 permeability of 3.70 barrers and H_2 permeability of 44.3. Meanwhile, it still maintained the higher gas permselectivity even at 100 °C, providing a promising candidate used as high-temperature gas membrane material.

References and Notes

- (1) Spillman, R. W. *Chem. Eng. Prog.* **1989**, 85, 41.
- (2) Gardner, R. J.; Crane, R. A.; Hannan, J. F. *Chem. Eng. Prog.* **1977**, 73, 76.
- (3) Mazur, W. H.; Chan, M. C. *Chem. Eng. Prog.* **1982**, 78, 38.
- (4) Usenko, K. A.; Springer, J.; Privalko, V. *J. Polym. Sci., Polym. Phys. Ed.* **1999**, 37, 2183.
- (5) Dorkenoo, K. D.; Pfromm, P. H.; Rezac, M. E. *J. Polym. Sci., Polym. Phys. Ed.* **1998**, 36, 797.
- (6) Shigetoshi, M.; Hiroki, S.; Tsutomu, N. *J. Membr. Sci.* **1998**, 141, 21.
- (7) Pixton, M. R.; Paul, D. R. *Macromolecules* **1995**, 28, 8277.
- (8) McHattie, J. S.; Koros, W. J.; Paul, D. R. *J. Polym. Sci., Polym. Phys. Ed.* **1991**, 29, 731.
- (9) Sheu, F. R.; Chern, R. T. *J. Polym. Sci., Polym. Phys. Ed.* **1989**, 27, 1121.
- (10) Stern, S. A.; Mi, Y.; Yamamoto, H. *J. Polym. Sci., Polym. Phys. Ed.* **1989**, 27, 1887.
- (11) Chen, T. L.; Yuan, Y. G.; Xu, J. P. Chinese patent, 1,038,098, 1988.
- (12) Aitken, C. L.; Koros, W. J.; Paul, D. R. *Macromolecules* **1992**, 25, 3424.
- (13) Muruganandam, N.; Koros, W. J.; Paul, D. R. *J. Polym. Sci., Polym. Phys. Ed.* **1987**, 25, 1999.
- (14) Jia, L. D.; Xu, J. P. *Polym. J.* **1991**, 23, 417.
- (15) Liu, W. Y.; Wang, Z. G.; Chen, T. L.; Xu, J. P. *Proceedings of the 1990 International Membrane and Membrane Processes*, Chicago, IL, 1990; p 836.
- (16) Wang, Z. G.; Chen, T. L.; Xu, J. P. *J. Appl. Polym. Sci.* **1997**, 64, 1725.
- (17) Wang, Z. G.; Chen, T. L.; Xu, J. P. *J. Appl. Polym. Sci.* **1997**, 63, 1127.
- (18) Sugden, S. *J. Chem. Soc.* **1927**, 1786.
- (19) Liu, W. Y.; Chen, T. L.; Xu, J. P. *J. Membr. Sci.* **1990**, 53, 203.
- (20) Xu, J. P.; Wang, Z. G.; Chen, T. L. *ACS Symp. Ser.* **1999**, 733, 269.
- (21) Jeans, J. *An Introduction to the Kinetic Theory of Gases*, Cambridge University Press: London, 1982; p 183.
- (22) Breck, D. W. *Zeolite Molecular Sieves*, John Wiley & Sons: New York, 1994; p 636.
- (23) Reid, R. C.; Pransnitz, J. M.; Sherwood, T. K. *The Properties of Gas and Liquids*, McGraw-Hill: New York, 1977; p 678.
- (24) Amerongen, G. J. *J. Appl. Phys.* **1946**, 17, 972.
- (25) Suwandi, M. S.; Stern, S. A. *J. Polym. Sci., Polym. Phys. Ed.* **1973**, 11, 663.
- (26) Shah, V. M.; Hardy, B. J.; Stern, S. A. *J. Polym. Sci., Polym. Phys. Ed.* **1986**, 24, 2033.
- (27) VanAmerongen, G. J. *Rubber Chem. Technol.* **1964**, 37, 1065.
- (28) Ghosal, K.; Chern, R. T.; Freeman, B. D.; Daly, W. H.; Negulesco, I. I. *Macromolecules* **1996**, 29, 4360.
- (29) Koros, W. J.; Fleming, G. K.; Jordan, S. M. *Prog. Polym. Sci.* **1988**, 13, 339.
- (30) Wang, Z. G. Doctoral Dissertation, CIAC CAS, Changchun, 1994.
- (31) Van Krevelen, D. W.; Hoftyzer, P. J. *Properties of Polymers*, Elsevier: New York, 1976.
- (32) Stannett, V. T. *Diffusion in Polymers*; Wiley and Sons, New York, 1971; Chapter 2.
- (33) Meares, P. *J. Am. Chem. Soc.* **1954**, 76, 3415.
- (34) Meares, P. *Diffusion of Gases and Vapors in Polymers. In Polymers: Structure and Bulk Properties*; D. Van Nostrand: London, 1965; Chapter 12.
- (35) Kim, T. H.; Koros, W. J.; Husk, G. R.; O'Brien, K. C. *J. Membr. Sci.* **1988**, 37, 45.
- (36) Hwang, S. T.; Choi, C. K.; Kammermeyer, K. *Sep. Sci.* **1974**, 9, 461.
- (37) Nakamura, A.; Kusuki, Y.; Nagagawa, K. *Proceedings of the 1987 International Conference of Membrane*; Tokyo, 1987; p 560.
- (38) Jia, L. D.; Xu, J. P. *Polym. J.* **1991**, 23, 417.
- (39) Yasuda, H.; Stannett, V. *Polymer Handbook*, 2nd ed.; Wiley: New York, 1975.
- (40) Paleo, A. C.; Muruganandam, N.; Paul, D. R. *J. Polym. Sci., Polym. Phys. Ed.* **1989**, 27, 2385.
- (41) Fu, H. Y.; Jia, L. D.; Xu, J. P. *J. Appl. Polym. Sci.* **1994**, 51, 1405.

MA9921807